Realizing the Potential of Physics-Informed Neural Network in Modelling Laser Drilling Process

Zahra Kheirandish[*1] and Wolfgang Schulz[1, 2]

[1]*NLD, RWTH Aachen University, Aachen, Germany*
[2]*Fraunhofer ILT, Aachen, Germany*
[*]*Corresponding author's e-mail: zahra.kheirandish@nld.rwth-aachen.de*

This research introduces a novel paradigm by integrating physics-based models with neural networks, forming a cohesive and adaptive framework for laser drilling. The Physics-Informed Neural Network (PINN) leverages the underlying physical principles governing laser-material interactions to enhance the predictive accuracy of drilling outcomes. Through meticulous training on diverse datasets encompassing material properties, laser parameters, and resultant hole geometries, the PINN model exhibits a remarkable ability to generalize across varied conditions. Here, the Artificial Neural Network's (ANN) inputs are spatial and temporal coordinates inside the domain, on the boundaries and at initial moment. The output is the shape of laser drilled hole. During the training step, the output values, and their derivatives w.r.t. inputs are calculated and afterwards they are used to evaluate the loss value. Through the gradient- based optimization method, the weights of network are changed to reach minimum loss value. The trained model predicts the unknown coefficient in the physical governing equation, which here is ablation threshold intensity. Our study investigates the effectiveness of the PINN approach in optimizing laser drilling parameters and achieving superior accuracy. We demonstrate its robustness in predicting drilling outcomes for different laser configurations. This research contributes not only to the advancement of laser precision microfabrication but also to the broader field of computational physics. By seamlessly integrating data-driven approaches with fundamental physical insights, the PINN methodology offers a transformative pathway to optimize laser drilling processes, paving the way for enhanced efficiency and quality in microfabrication applications. The insights presented herein promise to shape the future of laser microfabrication, fostering innovation and pushing the boundaries of precision engineering.
Keywords: laser drilling, PINN model, physics-informed neural network, physics-based deep learning

1. Introduction

Laser drilling process involves complex physical interactions, including thermal, mechanical, and optical phenomena, often described by nonlinear partial differential equations (PDEs). Traditional computational methods, while powerful, can be computationally expensive or may struggle with the multiscale and multiphysics aspects of laser processes [1, 2, 3].

Physics-Informed Neural Networks (PINNs) integrate physical principles, typically in the form of differential equations, into the architecture or loss function of the artificial neural network. This ensures that the solutions provided by the network comply with the underlying physical laws governing the system.

It can be particularly advantageous in scenarios where data is scarce or expensive to obtain, as the network can be trained on a combination of sparse data and physical laws, reducing the reliance on extensive datasets. It offers a promising alternative by providing a framework to model these complex interactions efficiently.

Very early research work on capabilities of PINNs was conducted to solve *Schrödinger equation* and *Allen–Cahn equation*, and also to find unknown parameters in *Navier–Stokes equation* and *Korteweg–de Vries equation* [4]. Later it is employed to find unknown parameters in equations of linear elastostatics [5]. Recently, it is used to approximate unknown parameters of displacement in the elastic body with crack [6]. This model can enhance fatigue crack growth simulation and life prediction of structures.

In terms of application of PINNs in Laser manufacturing problems, a finite element model is combined with an Artificial Intelligence-powered PDE solver, PINNs, to speed up simulating selective laser sintering process and also to optimize the manufacturing process [7].

It is also used to predict 3-dimensional temperature field in laser metal deposition process; here, the loss function is constructed of residuals of heat conduction, convection and radiation equation, and training step does not require any labeled temperature data [8]. In Addition, to speed up computation time in calculating temperature profile of laser powder bed fusion process, parametric PINNs are established; the computation time of trained model is several orders of magnitude shorter than finite element model [9].

PINNs can be extended to solve inverse problems, where the objective is to infer underlying physical parameters or sources from observed data. The ability of PINNs to provide real-time predictions makes them suitable for monitoring and controlling laser manufacturing processes. To predict temperature change history and to find unknown material properties and parameters of additive manufacturing process, the thermal measurement of infrared camera is combined with a PINNs model; this hybrid model predicts accurately the unknowns

and is capable to be used in real-time processes[10].

As it is evident, the application of physics-informed neural networks in laser manufacturing is an exciting frontier that combines the strengths of machine learning and physical sciences. Therefore, in this research work, to show extra the potential of physics-informed neural network in laser manufacturing processes, the long-pulse laser drilling process is chosen as the use case.

It is aimed to produce more accurate and physically consistent predictions even with limited data by incorporating physical laws into ANN. Our approach is structured as follows. The succeeding main section explains the structure of physics-informed neural networks. Section 3 then introduces the governing differential equation of long-pulse laser drilling model. Section 4 demonstrates the programming technique and the methodology as well as operation of finding and discovering solutions. Finally, Section 5 concludes the outcomes.

2. Physics-Informed Neural Networks: PINNs

Physics-Informed Neural Networks, are constructed through integrating physical laws, described by partial differential equations (PDEs), directly into the training process of the neural networks. These equations constrain the training process to ensure the neural network's predictions adhere to physical laws.

A typical PINNs architecture consists of a feedforward artificial neural network with several layers and activation functions, as shown in fig. 1. The input to the network can include spatial coordinates (x) and time (t) while the output represents the solution to the differential equation (u^p). The governing equation and its initial and boundary conditions are $f_{pde}(u, u_x, u_{xx}, u_t) = f_0$ and $f_b(u, u_x, u_{xx}, u_t) = f_{0,b}$, respectively.

The derivatives of the solution i.e., u_x, u_{xx}, and u_t are computed by algorithmic differentiation (AD) technique which is an automatic method for computing gradients of numerical algorithms [11].

In this model, the loss function is augmented to include terms that enforce the physical constraints. This typically calculate mean squared errors (MSE) and involves data loss MSE_u and physical loss MSE_f. The former measures the error between the network's predictions (u^p) and any available data points or observations (u^t). The latter ensures the network's output satisfies the differential equations. This is done by computing the residuals of the differential equations (f_{pde} and f_b) using automatic differentiation and including them in the loss function.

During training, the network adjusts its weights to minimize the combined loss (data loss + physics loss), thus learning to produce solutions that are consistent with both the observed data and the underlying physical laws

The depicted algorithm in fig. 1 conducts to data-driven solution. However, the PINNs has more potentials. It can be used to find unknown parameters of governing equations as well, as shown in fig. 2. To do so, the network shall predict the solution of the differential equation as well as the unknown parameters. This way of establish the algorithm leads to data-driven discovery of PDEs. To find the unknown parameters, one needs knowledge about ground truth values
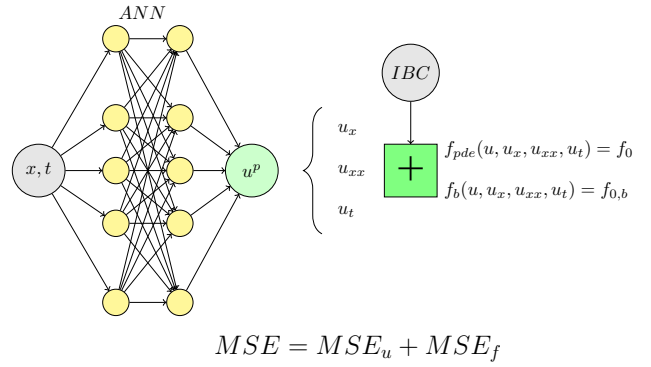

$$MSE = MSE_u + MSE_f$$

Fig. 1 Typical physics-informed neural networks architecture.

as well. This knowledge can be obtained from available experimental or numerical results to compare with the predicted results. Afterwards, the loss function is constructed of two mean squared errors, i.e., mean squared error of predictions and the residual function.
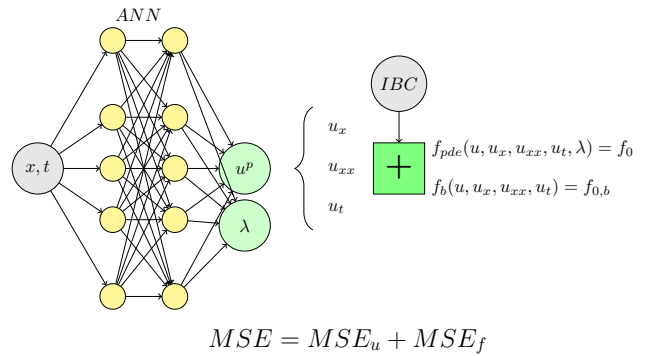

$$MSE = MSE_u + MSE_f$$

Fig. 2 Customized physics-informed neural networks architecture.

This approach represents a powerful approach to solve complex problems where traditional methods might struggle, providing a bridge between machine learning and physical sciences. A strong feature of this approach is that it requires less observational data compared to purely data-driven models because the physical laws provide additional information.

3. Long-pulse laser drilling equation

When it comes to long-pulse laser drilling, the dominant thermal process is melting and material is removed when specific amount of energy is absorbed; this value is called ablation intensity threshold [12]. By knowing the ablation intensity threshold one can write an asymptotic time-dependent equation to approximate the shape of drilling hole, as will be explained in this section.

Assume that the laser beam is irradiated to the workpiece surface with inclination angle θ_{inc}. If $\mu = \cos(\theta_{inc})$ the following relation should read to ablation take place:

$$\mu A(\mu) I(x, z) = \tilde{I}_{\text{thr}}. \tag{1}$$

Here, $I(x, z)$ and $A(\mu)$ are power intensity distribution and the absorption coefficient, respectively. By plotting the

$\mu A(\mu)$, one can find out that this term can be approximate with a linear relation $G\mu$ [12]; G is a constant coefficient.

Through defining $I_{\text{thr}} = \tilde{I}_{\text{thr}}/G$ and using the trigonometry relation $1 + \tan(x)^2 = \frac{1}{\cos(x)^2}$, we approximate the inclination of the drill wall as below:

$$\frac{dz_{\text{r,l}}}{dx} = \pm\sqrt{\left(\frac{I(x, z_{\text{r,l}})}{I_{\text{thr}}}\right)^2 - 1}. \qquad (2)$$

For a specific ablation thickness (Δz), the next x-coordinate of the wall is calculated, as:

$$x_i = x_{i-1} + \left(\frac{dz}{dx}\right)^{-1} \Delta z. \qquad (3)$$

The Gaussian distribution is assumed for the beam optical intensity $I(x, z)$:

$$I(x, z) = I_0 \times \left(\frac{w_0}{w(z)}\right)^2 \times e^{\left(-2\left(\frac{x}{w(z)}\right)^2\right)}, \qquad (4)$$

while beam caustic function is $w(z) = w_0\sqrt{1 + (\frac{z-z_0}{z_R})^2}$. The focal beam radius is w_0. As it is seen, the spatial shape of the beam is characterized by beam focal position z_0 and Rayleigh length z_R, precisely, the propagation characteristic length of the beam. The latter is described as bellow:

$$z_R = \frac{\lambda}{\pi}\frac{F^2}{K}. \qquad (5)$$

As shown, the Rayleigh length depends on the focal number $F = \frac{z_f}{D}$ and beam quality factor $K = \frac{\lambda}{\pi}\frac{1}{\theta w_0}$. Here, D is the illuminated diameter of the focusing lens with focal length z_f and $\theta = w_0/z_R$ is the far-field divergence angle of the beam.

If P_l is defined as laser beam pulse power, the amplitude of optical intensity is calculated as below:

$$I_0 = 2P_l/(\pi w_0^2). \qquad (6)$$

When the first-order differential equation (i.e., eq. (2)) is solved for z, the (x, z) coordinate points of the borehole's wall are obtained. This numerical model needs to be calibrated experimentally. Through calibration, the ablation intensity threshold is varied until the calculated spatial shape of the borehole fits the manufactured borehole.

Since, influences of complex phenomena while laser drilling process, i.e., ionization, evaporation, melting, melt flow, and condensation are approximated and summed up in the threshold value, this model is called asymptotic threshold model. For drilling through AISI 304 stainless steel, the ablation threshold value is $2.25 \times 10^5 J/m^2$.

4. Data exploration and exploitation via PINNs

As explained in section 2, the PINNs can help us in finding data-driven solutions (data exploration) and data-driven discovery (data exploitation) of PDEs. The former is solution of PDEs; for given fixed parameters and coefficients of mathematical model, what can be the unknown state of variables. On the other hand, the latter is learning the system

identification; the parameters and coefficients of the mathematical model are unknown, what are acceptable values for best describe the observed data.

In this study, a 3-layer artificial neural network with 30 neurons in each layer is employed, and the governing equation is integrated into the loss function. To let this network to learn and model complex relationships within the data, appropriate non-linear activation function shall be introduced to it. In fact, without non-linearity, a neural network with multiple layers would be equivalent to a single-layer network, as the composition of linear functions is itself a linear function.

Therefore, activation functions enable neural networks to approximate complex function so that by applying non-linear transformations at each layer, the network can learn and represent a wide variety of functions. Properly chosen activation function ensures gradients are not too large or too small, which aids in effective training using gradient-based optimization techniques like back propagation [13]. Here, the $\tanh(x) = \frac{e^x - e^{-x}}{e^x + e^{-x}}$ function is used. It squashes input values to a certain range (e.g.,-1 to 1) which helps in stabilizing the learning process.

To train proposed PINNs, the gradient of the loss function shall be calculated; herein the algorithmic differentiation aids by exploiting the chain rule of differential calculus [11]. In the present analysis, an ANN model is built through *TensorFlow* [14] which is a well-known open-source machine learning platform. This platform benefits from the AD for training ANNs which can compute the gradients of differentiable expressions.

Adaptive moment estimation (Adam) [15] approach is the optimization strategy, which is a gradient-based technique and serves efficiently in training ANNs. It traces the gradient of the entire training set downhill until it reaches the minimum while the optimization procedure is controlled by learning rate (α). The utilized momentum method is favored because it directs faster the gradient downturn in the relevant direction and lessens oscillations. In this study the learning rate is set 10^{-3}.

Let's start with finding data-driven solutions of eq. (2) which is a nonlinear differential equation. Here, the goal is to find the shape of drill hole by means of PINNs. Firstly, the residual function shall be specified, which is as bellow for left-side wall:

$$f(x, z) = \frac{dz_{\text{r,l}}}{dx} + \sqrt{\left(\frac{I(x, z_{\text{r,l}})}{I_{\text{thr}}}\right)^2 - 1}. \qquad (7)$$

For a given I_{thr} and (x), an artificial neuronal network is trained such that residual of governing equation is minimized during training. The unknown variable is z positions of drill wall for certain x. The derivative of z is calculated by means of automatic differentiation. In the next step, this approximation is inserted to eq. (7) to obtain a physics-informed neural network.

The data pipeline is depicted in fig. 3. The loss function is the mean square error of residual function and the weights and bias of ANN are modified in each epoch.

In fig. 4 the mean squared error of training is depicted; after enough training epochs, it reaches 10^{-2} which is an
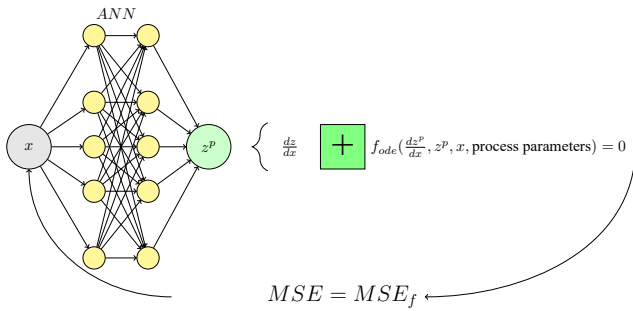
Fig. 3 Physics-informed neural networks architecture for finding Physics-driven model solution.

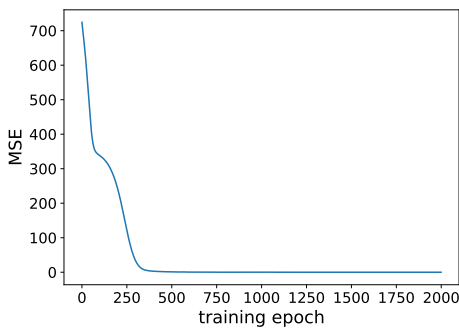acceptable value for the residual function.

Fig. 4 MSE of training. A [3×30] artificial neural network with tanh activation function is employed. The training learning rate is 10e-3.

The comparison between the predicted shape of drill wall by PINNs model and outcomes of numerical solution, represents a very close results. This agreement is shown in fig. 5. Here, the expected shape of drill wall is obtained by means of numerical solution of eq. (2). This asymptotic model is developed by [12]. To check the valiity and accuracy of the model, he compared it with actual experimental data; athe very good agreement between experimental and numerical solution is observed.
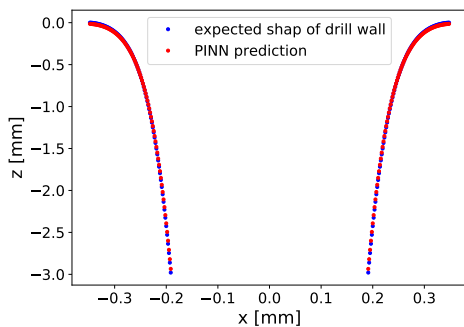

Fig. 5 Comparison of predictions of PINN model and numerical solution of laser borehole by eq. (7).

As said before, PINNs advantage is more evident when it comes to data-driven discovery, that means finding unknown

coefficient or parameters in the equation. One can do several experiments to learn the relations and fins the value, however, wiser approach could be employing proposed method. Again, we start with the residual function eq. (7). Given noisy information about measurements of drill hole shape, we aim to approximate I_{thr}.

We approach the problem by approximating $z(x)$ and I_{thr} with a deep neural network. The data pipeline is shown fig. 6.
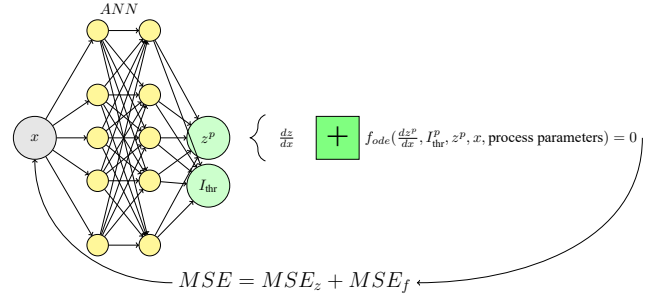

Fig. 6 Physics-informed neural networks architecture for finding data-driven discovery.

Here, in order to find out the unknown parameter we need to have ground truth of $z(x)$ as well. That means, one can use available experimental or numerical results to compare with the predicted results. Herein, the loss function is constructed of two mean squared errors. They calculate the mean square error of predicted $z(x)$ and the residual function.

The predicted shape of drill wall via data-discovery PINNs is depicted in fig. 7. Fortunately, the predicted values show a very good agreement with expected shape achieved via numerical simulation.
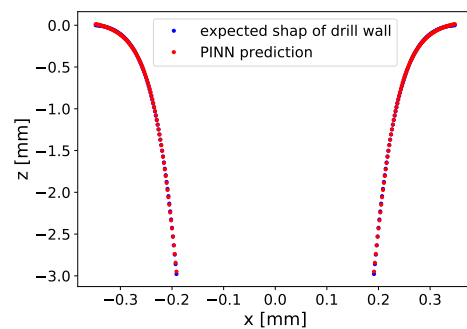

Fig. 7 Comparison of predictions and numerical solution of eq. (7) for the second PINNs model.

Last but not least, the predicted value for unknown parameter of model, i.e., I_{thr}, is depicted in fig. 8. Expected value for I_{thr} is 2.25×10^5 and as it is shown the predicted value is 2.2453×10^5, that is a very acceptable prediction.

As it is seen, PINNs offer a versatile and robust framework for integrating domain knowledge into machine learning models, significantly enhancing their predictive power and generalization capabilities. This is what makes them an invaluable tool for advancing scientific discovery and engineering innovation.
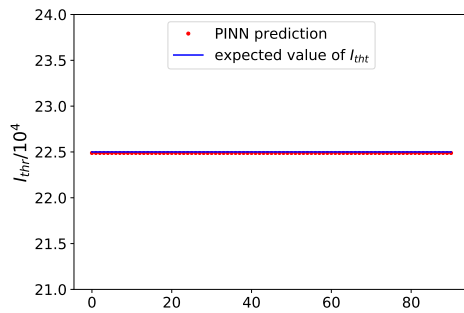
Fig. 8 Prediction of unknown parameter of eq. (7) via the second PINNs model.

5. Conclusion

As shown, the application of physics-informed neural networks in laser manufacturing is an exciting frontier that combines the strengths of machine learning and physical sciences. It is seen that PINNs can help us in finding data-driven solutions as well as data-driven discovery of nonlinear PDEs.

In this research work, the first proposed approach helps us find the unknown state of variables of PDE, i.e., z-position of drill wall, for given fixed parameters and coefficients of mathematical model. On the other hand, the second algorithm lets us learn the system identification which is intensity threshold value of laser ablation model as well as to predict shape of drill wall. The predictions of both models show a very good agreement with expected results.

It can be concluded that as research progresses, PINNs will play a significant role in enhancing the efficiency, precision, and capabilities of laser manufacturing processes, driving innovations in manufacturing technologies.

It is worth to mention that while PINNs hold substantial promise for advancing laser manufacturing technologies, several challenges remain. These include the need for improved methods to handle complex geometries, the integration of multiple physical phenomena at different scales, and the development of more efficient training algorithms to handle the computational complexity of high-dimensional problems. Therefore, our future research will focus on enhancing the interpretability and robustness of PINNs, ensuring that they can be reliably applied in real industrial settings.

References

[1]   W. Schulz, U. Eppelt, and R. Poprawe: J. Laser Appl., 25, (2013) 012006.

[2]   C. Heinigk, T. Barthels, M. Nießen, and W. Schulz: J. Laser Micro Nanoeng., 16, (2021) 144.

[3]   C. Heinigk, T. Barthels, W. Schulz, and M. Nießen: Opt. Eng., 61, (2022) 095103.

[4]   M. Raissi, P. Perdikaris, and G. E. Karniadakis: J. Comput. Phys., 378, (2019) 686.

[5]   E. Haghighat, M. Raissi, A. Moure, H. Gomez, and R. Juanes: Comput. Methods Appl. Mech. Eng., 379, (2021) 113741.

[6]   Z. Chen, Y. Dai, and Y. Liu: Int. J. Fatigue, 186, (2024) 108382.

[7]   H.-P. Yeh, M. Bayat, A. Arzani, and J. H. Hattel: Appl. Math. Model., 130, (2024) 693.

[8]   S. Li, G. Wang, Y. Di, L. Wang, H. Wang, and Q. Zhou: Eng. Appl. Artif. Intell., 120, (2023) 105908.

[9]   E. Hosseini, P. Scheel, O. Müller, R. Molinaro, and S. Mishra: Comput. Methods Appl. Mech. Eng., 410, (2023) 116019.

[10]   S. Liao, T. Xue, J. Jeong, S. Webster, K. Ehmann, and J. Cao: Comput. Mech., 72, (2023) 499.

[11]   A. G. Baydin, B. A. Pearlmutter, A. A. Radul, and J. M. Siskind: J. Mach. Learn. Res., 18, (2018) 1.

[12]   T. Hermanns: "Interaktive Prozesssimulation für das industrielle Umfeld am Beispiel des Bohrens mit Laserstrahlung", (RWTH Aachen University, 2018) p.46.

[13]   I. Goodfellow, Y. Bengio, and A. Courville: "Deep Learning", (MIT Press, 2016) p.302.

[14]   T. Developers: "TensorFlow: Large-Scale Machine Learning on Heterogeneous Systems", URL: https://www.tensorflow.org/.

[15]   D. P. Kingma and J. Ba: Proc. ICLR2015, (2015) 1.